Received: 4 February 2020 | Accepted: 21 May 2020

DOI: 10.1002/jcp.29839

ORIGINAL RESEARCH ARTICLE

Journal of Cellular Physiology WILEY

Cholic acid and deoxycholic acid induce skeletal muscle atrophy through a mechanism dependent on TGR5 receptor

Johanna Abrigo[1,2,3] | Francisco Gonzalez[1,2,3] | Francisco Aguirre[1,2,3] | Franco Tacchi[1,2,3] | Andrea Gonzalez[1,2,3] | María Paz Meza[1,2,3] | Felipe Simon[2,4,5] | Daniel Cabrera[6,7] | Marco Arrese[6] | Saul Karpen[8] | Claudio Cabello-Verrugio[1,2,3]

[1]Laboratory of Muscle Pathology, Fragility suand Aging, Department of Biological Sciences, Faculty of Life Sciences, Universidad Andres Bello Universidad Andres Bello, Santiago, Chile

[2]Millennium Institute on Immunology and Immunotherapy, Santiago, Chile

[3]Center for the Development of Nanoscience and Nanotechnology (CEDENNA), Universidad de Santiago de Chile, Santiago, Chile

[4]Millennium Nucleus of Ion Channels-Associated Diseases (MiNICAD), Universidad de Chile, Chile

[5]Laboratory of Integrative Physiopathology, Department of Biological Sciences, Faculty of Life Sciences, Universidad Andres Bello Universidad Andres Bello, Santiago, Chile

[6]Departamento de Gastroenterología, Escuela de Medicina-Centro de Envejecimiento y Regeneración (CARE), Facultad de Ciencias Biológicas, Pontifica Universidad Católica de Chile, Santiago, Chile

[7]Facultad de Ciencias Médicas, Universidad Bernardo OHiggins, Santiago, Chile

[8]Department of Pediatrics, Emory University School of Medicine, Atlanta, Georgia

Correspondence
Claudio Cabello-Verrugio, Laboratory of Muscle Pathology, Fragility and Aging, Department of Biological Sciences, Faculty of Life Sciences, Universidad Andres Bello, 8370146 Santiago, Chile.
Email: claudio.cabello@unab.cl

Funding information
BASAL Grant CEDENNA, Grant/Award Number: AFB180001; Programa de Cooperación Científica ECOS-CONICYT, Grant/Award Number: C16S02; Millennium Institute on Immunology and Immunotherapy, Grant/Award Number: P09-016-F; CONICYT Ph.D. scholarship, Grant/Award Number: 21161353; Nucleus of Ion Channels-Associated Diseases, Grant/Award Number: MiNICAD; Comisión Nacional de Investigación, Ciencia y Tecnología (CONICYT), Grant/Award Number: AFB170005, CARE Chile-UC; National Fund for Science and Technological Development, Grant/Award Numbers: Fondecyt 11171001, Fondecyt 1161288, Fondecyt 1161646, Fondecyt 1191145

Abstract

Skeletal muscle atrophy is characterized by the degradation of myofibrillar proteins, such as myosin heavy chain or troponin. An increase in the expression of two muscle-specific E3 ligases, atrogin-1 and MuRF-1, and oxidative stress are involved in muscle atrophy. Patients with chronic liver diseases (CLD) develop muscle wasting. Several bile acids increase in plasma during cholestatic CLD, among them, cholic acid (CA) and deoxycholic acid (DCA). The receptor for bile acids, TGR5, is expressed in healthy skeletal muscles. TGR5 is involved in the regulation of muscle differentiation and metabolic changes. In this paper, we evaluated the participation of DCA and CA in the generation of an atrophic condition in myotubes and isolated fibers from the muscle extracted from wild-type (WT) and TGR5-deficient ($TGR5^{-/-}$) male mice. The results show that DCA and CA induce a decrease in diameter, and myosin heavy chain (MHC) protein levels, two typical atrophic features in C_2C_{12} myotubes. We also observed similar results when INT-777 agonists activated the TGR5 receptor. To evaluate the participation of TGR5 in muscle atrophy induced by DCA and CA, we used a culture of muscle fiber isolated from WT and $TGR5^{-/-}$ mice. Our results show that DCA and CA decrease the fiber diameter and MHC protein levels, and there is an increase in atrogin-1, MuRF-1, and oxidative stress in WT fibers. The absence of TGR5 in fibers abolished all these effects induced by DCA and

CA. Thus, we demonstrated that CS and deoxycholic acid induce skeletal muscle atrophy through TGR5 receptor.

KEYWORDS
autophagy, bile acids, muscle atrophy, muscle wasting, ROS, TGR5 receptor, ubiquitin-proteasome system

1 | INTRODUCTION

Several muscular pathologies are characterized by skeletal muscle atrophy, which is the loss of muscle mass and function (Cao, Li, Dai, Li, & Yang, 2018; Ding, Dai, Huang, Xu, & Zhong, 2018). Some features of muscle atrophy are a decline in muscle strength, decrease of fiber diameter, and loss of myofibrillar proteins (i.e., myosin heavy chain [MHC] and troponin; Cabello-Verrugio, Rivera, & Garcia, 2017; Dumitru, Radu, Radu, & Cretoiu, 2018). The primary mechanism responsible for protein breakdown in the muscle during atrophy is the ubiquitin-proteasome system (UPS), which is increased under atrophic conditions, as evidenced by an increase in the gene expression of two muscle-specific E3-ubiquitin ligases, atrogin-1/MAF-bx and MuRF-1/TRIM63 (Khalil, 2018). More important, MHC and troponin are targets of MuRF-1 and atrogin-1 and further degraded via the proteasome (Bilodeau, Coyne, & Wing, 2016). Besides, autophagy, a process deregulated in muscle atrophy, is involved in the catabolic pathway in skeletal muscle (Call & Nichenko, 2020; Sandri, 2010, 2013). Another intracellular event that is evident in muscle atrophy is the presence of oxidative stress. In general, the causes of oxidative stress are an increase in the production of reactive oxygen species (ROS) and/or a decrease of the antioxidant mechanism in cells that cause cellular damage (Abrigo et al., 2018).

Among the causes of muscle atrophy are aging, immobilization, sepsis, and long-term conditions, such as chronic liver diseases (CLD; Abrigo, Simon, Cabrera, Vilos, & Cabello-Verrugio, 2019; Cao et al., 2018). Patients with CLD present with a muscle weakness named sarcopenia (Ponziani & Gasbarrini, 2017). Its influence on mortality has defined the importance of sarcopenia in the health of patients with CLD after a liver transplant (Dasarathy, 2013; Englesbe et al., 2010; Tsien et al., 2014). The intracellular mechanisms involved in CLD-induced weakness have been studied for our group in murine models of CLD by observing the participation of UPS, oxidative stress, and apoptosis (Abrigo, Marin, et al., 2019; Campos et al., 2018). One of the soluble mediators elevated in the plasma in CLD is the bile acids (M. J. Kim & Suh, 1986; Luo et al., 2018). The most relevant bile acids in CLD are cholic acid (CA) and deoxycholic acid (DCA; Kobayashi et al., 2017).

Bile acids are not only involved in the digestive function but also as signaling molecules with extrahepatic functions in the small intestine, brown adipose tissue, macrophages, and skeletal muscle (Dossa et al., 2016; Kars et al., 2010; T. Li & Apte, 2015; T. Li & Chiang, 2015; Qi et al., 2015). These functions are dependent on the activation of two receptors for bile acids: intracellular farnesoid X receptor (FXR) and plasma membrane G-protein-coupled TGR5 receptor (Deutschmann et al., 2018; Kawamata et al., 2003; Keitel, Stindt, & Haussinger, 2019; Makishima et al., 1999). Several tissues express FXR, such as the liver, heart, intestine, and adipose tissue (Shin & Wang, 2019). Skeletal muscle express TGR5 receptor, and the contractile activity and the unfolded protein response (UPR) are regulators of its expression (Sasaki et al., 2018). The function described for TGR5 in skeletal muscle is mainly the regulation of muscle differentiation (Sasaki et al., 2018). Besides, bile acids induce the deiodinase 2 expression, which produces the T4 to T3 transformation, and also regulate insulin resistance through a mechanism dependent on TGR5 (Huang et al., 2019; Watanabe et al., 2006). Interestingly, only one unique study has shown an association between serum bile acids and skeletal muscle volume during non-alcoholic fatty liver disease (Kobayashi et al., 2017).

In this study, we analyzed the role of CA and DCA in the induction of skeletal muscle atrophy and the participation of TGR5 receptor.

2 | MATERIALS AND METHODS

2.1 | Animals

C57BL/6J Gpbar1$^{-/-}$ mice (referred to in this study as TGR5$^{-/-}$ mice) and their C57BL/6J WT littermates were kindly donated by Dr. Auwerx (Laboratory of Integrative and Systems Physiology, École Polytechnique Fédérale de Lausanne, Switzerland) to Dr. Marco Arrese. The animals were maintained in our animal facility at Universidad Andres Bello. The study was performed on randomized male 12–16-week-old mice. All applicable international, national, and institutional guidelines for the care and use of animals were followed. All procedures performed in this study that involves animals followed the ethical standards. The Animal Ethics Committee belongs to the Universidad Andrés Bello formally approved these procedures (Approval number 007/2016).

2.2 | Cell cultures

The skeletal muscle cell line C_2C_{12} (American Type Culture Collection) was grown and differentiated until Day 5, as previously described (Cabello-Verrugio et al., 2011; Droguett, Cabello-Verrugio, Santander, & Brandan, 2010; Painemal, Acuna, Riquelme, Brandan, &

Cabello-Verrugio, 2013). The myotubes were incubated with DCA, CA (Sigma-Aldrich), or INT-777 (MedChem) in the concentrations and times indicated in each figure. Myotubes were also incubated with INT-777 at 25 or 50 μM for the time indicated for each experiment. To measure autophagy markers, myotubes were incubated with bile acids for 8 hr. Specifically, to detect LC3II and LC3I, myotubes were pre-incubated with chloroquine (CQ; 50 μM; Sigma-Aldrich) for 5 min before bile acids and then co-incubated for a total of 8 hr.

2.3 | Cell viability

C_2C_{12} myotubes were incubated for 72 hr with the concentration of DCA and CA indicated in each figure. The cell viability was evaluated using the CCK-8 kit (Sigma-Aldrich) following the instructions of the manufacturer. The absorbance was measured at 450 nm.

2.4 | Isolation and culture of single-myofiber explants

Single myofibers were isolated from the extensor digitorum longus (EDL) muscles of C57BL/6J mice, as described by Pasut, Jones, and Rudnicki (2013). Briefly, the EDL muscle was dissected and digested in an F12 medium containing 750 U/ml collagenase type I (Worthington Biochemical) at 37°C for 1 hr with gentle agitation. Single myofibers were then carefully dissociated by flushing the muscle with F12-15% horse serum (HS). Single myofibers were extracted individually using a dissecting microscope and fire-polished pipettes and transferred serially into fresh F12-15% HS. Approximately 20–50 myofibers were transferred into 24-well plates covered with Matrigel (1:1 dilutes in F12) and incubated for 24 hr in a humidified, 37°C, 5% CO_2 incubator. The next day, the medium was aspirated and exchanged with fresh medium in which the different treatments were performed.

2.5 | Immunofluorescence microscopy

The location of MHC was analyzed by indirect immunofluorescence (Meneses et al., 2015). Briefly, C_2C_{12} myoblasts were grown and differentiated on glass coverslips and after respective treatments were fixed in 4% paraformaldehyde, permeabilized with 0.05% Triton X-100, and incubated for 1 hr with 1:100 mouse anti-MHC (MF-20; Developmental Studies, Hybridoma Bank, University of Iowa) in a buffer containing 50 mM Tris–HCl, pH 7.7; 0.1 M NaCl; and 1% bovine serum albumin. After antibody removal and several washes with the mentioned buffer, bound antibodies were detected by incubating the cells for 30 min with 1:100 affinity-purified Alexa Fluor dye-conjugated goat anti-mouse antibody (Life Technologies). For nuclear staining, the sections were incubated with 1 μg/ml Hoechst 33258 in phosphate-buffered saline (PBS) for 10 min. After rinsing, the sections were mounted with a fluorescent-mounting medium (Dako Corporation) under glass coverslips, viewed, and photographed with the Motic BA310 epifluorescence microscope (Motic, Hong Kong). The MF-20 hybridoma, monoclonal antibody developed by Fischman, D.A. was obtained from the Developmental Studies Hybridoma Bank, created by the NICHD of the NIH and maintained at The University of Iowa, Department of Biology, Iowa, IA.

2.6 | Measurement of myotube and isolated myofiber diameter

C_2C_{12} myotube and myofiber cultures were immunostained with anti-MHC. Photographs obtained of myotube or fiber immunofluorescent for MHC in different zones of the coverslip were analyzed. The minimal Feret diameters were measured (at three different points of each myotube or fiber) in a total of 80 myotubes from 10 random fields and in 20–30 myofibers from each

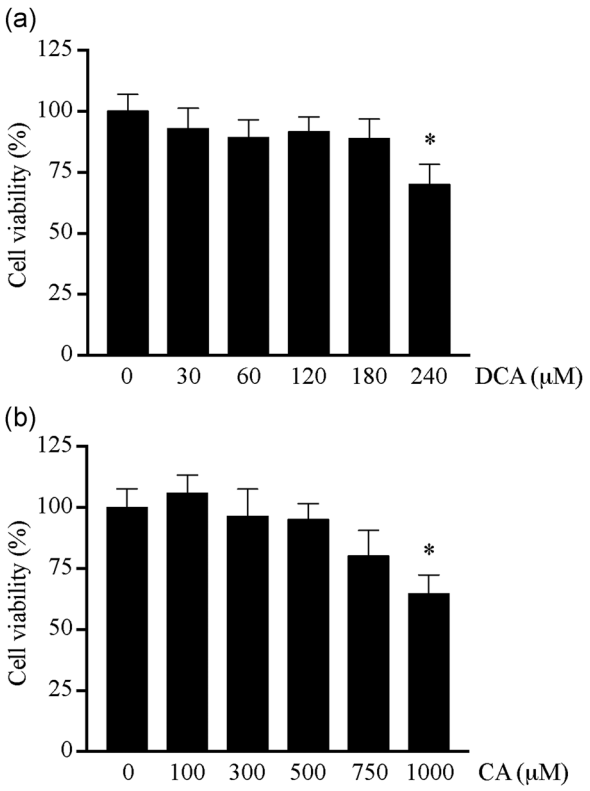

FIGURE 1 Cell viability in C_2C_{12} myotubes incubated with DCA and CA acids. C_2C_{12} myoblasts were differentiated for 5 days and then incubated with increasing concentrations of DCA (0 up to 240 μM) or CA (0 up to 1,000 μM) acids for 72 hr. Cell viability was evaluated through CCK-8 kit for DCA (a) and CA (b). The values indicate the percentage which is expressed as the mean ± *SD* of three independent experiments in triplicate (one-way ANOVA, post-hoc Bonferroni, $^*p < .05$ relative to the control). ANOVA, analysis of variance; CA, cholic acid; CCK-8, cell counting kit-8; DCA, deoxycholic acid

experimental condition in a blind fashion, using computerized image analysis (ImageJ, National Institutes of Health [NIH]). Myotubes were defined as all multinucleated (containing three or more nuclei) cells positive for MHC stain (Morales et al., 2015).

2.7 | Measurement of intracellular reactive oxygen species (ROS) levels

C_2C_{12} myotubes were cultured on glass coverslips and further treated with myostatin for 24 hr. At the end of this experiment, the cells were washed with Hank's Balanced Salt Solution and incubated with H2-DCF-DA for 30 min at 37°C. After two washes with Hank's Balanced Salt Solution and one wash with PBS, the cells were fixed with 4% paraformaldehyde for 10 min and washed with PBS. The cells were incubated with 1 μg/ml Hoechst 33258 in PBS for 10 min for nuclear staining. After rinsing, the cells were mounted with a fluorescent-mounting medium (Dako Corporation), viewed, and photographed with the Motic BA310 epifluorescence microscope (Motic, Hong Kong).

2.8 | Transient plasmid transfection

One microgram of pCre-luc, a plasmid reporter with Cre sites that respond to increases of cAMP (Invitrogen), and 0.02 μg of pRL-SV40 was used to co-transfect cells using 1 μl of LipofectAMINE 3000 in Opti-MEM I. After 6 hr, FBS was added to the medium and the cells were cultured for a further 12 hr. Then, the cells were differentiated for 4 days, and the treatments were performed as indicated in the figures. Dual-luciferase activity assays (Promega) were performed after 24 hr in a GloMax 20/20 luminometer (Promega).

2.9 | Immunoblot analysis

For the protein extracts, myotubes were homogenized in a radioimmunoprecipitation assay buffer with a cocktail of protease inhibitors and 1 mM of phenylmethylsulfonyl fluoride. Proteins were subjected to sodium dodecyl sulfate polyacrylamide gel electrophoresis, transferred onto polyvinylidene difluoride membranes (Millipore), and probed with mouse anti-MHC (1:3,000; MF-20,

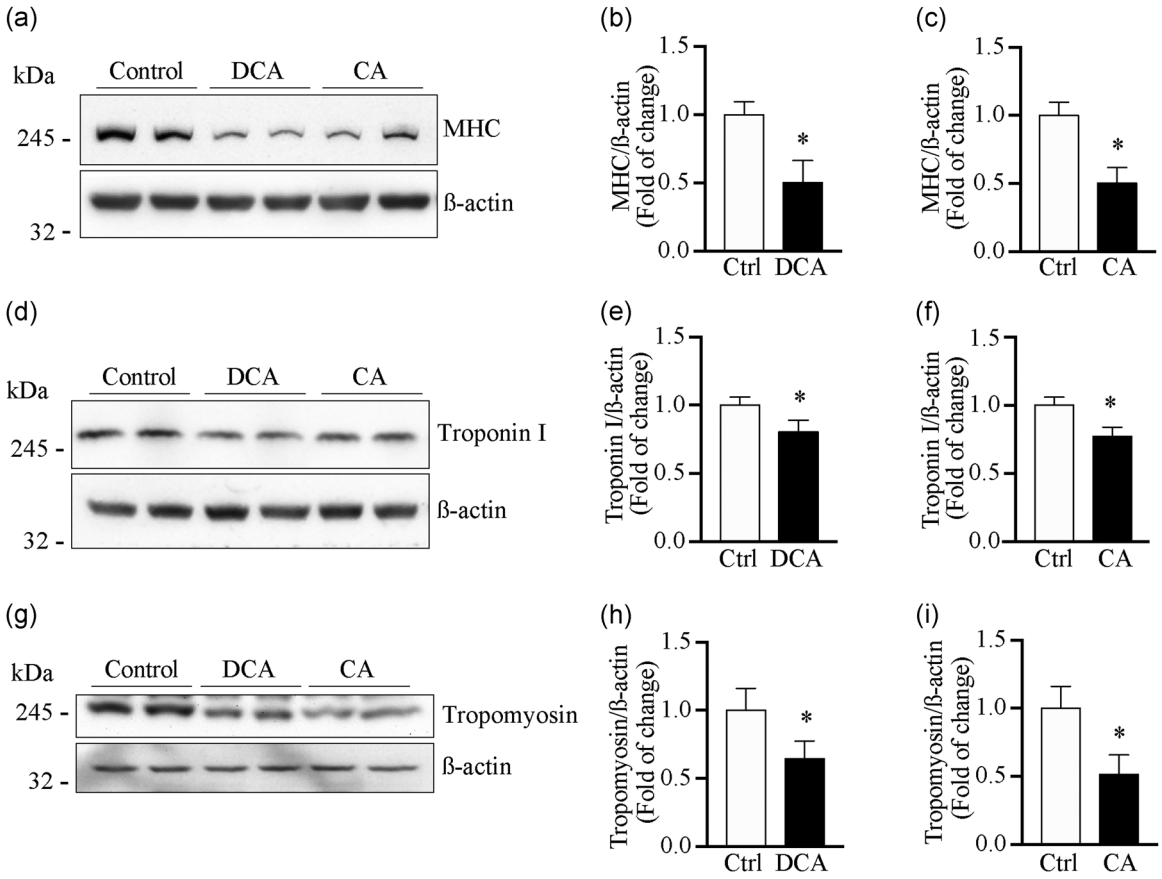

FIGURE 2 Myofibrillar protein levels are reduced by DCA and CA in C_2C_{12} myotubes. C_2C_{12} myoblasts differentiated for 5 days were incubated with DCA (120 μM) or CA (500 μM) for 72 hr. MHC (a), troponin I (d), and tropomyosin (g) protein levels were detected by western blot analysis, using β-actin as the loading control. Molecular weights are shown in kDa. Densitometric analysis for MHC (b,c), troponin I (e,f), and tropomyosin (h,i) are shown as a fold of change expressed as the mean ± *SD* of three independent experiments in triplicate (*t* test; $^*p < .05$ relative to the control). CA, cholic acid; DCA, deoxycholic acid; MHC, myosin heavy chain

Developmental Studies, Hybridoma Bank, University of Iowa), goat anti-4-hydroxynonenal (4-HNE; 1:1,000; Merck), rabbit anti-LC3B (1:1,000), rabbit anti-p62 (1:1,000; Cell Signaling Technology Inc.), rabbit anti-atrogin-1 (1:500), rabbit anti-MuRF-1 (1:500; ECM Biosciences), as well as rabbit anti-troponin I (1:1,000), rabbit anti-Iκ-B (1:5,000), and rabbit anti-β-actin (1:5,000; Santa Cruz Biotech). All immunoreactions were visualized by enhanced chemiluminescence (Thermo Fisher Scientific). Images were acquired using the Fotodyne FOTO/Analyst Luminary Workstation Systems (Fotodyne, Inc.). Densitometry analysis was determined by scanning immunoreactive bands, and intensity values were obtained for further normalization against the control group.

2.10 | Reverse-transcription and quantitative PCR

Total RNA was isolated from muscle cells C_2C_{12} and the liver using Chomczynski solution. cDNA was obtained from 2 μg of RNA by reverse transcription. The messenger RNA (mRNA) relative expression of FXR (forward, TGTGAGGGCTGCAAAGGTT; reverse, ACATCCC CATCTTGGAC) and TGR5 (forward, CAGGAGGCCATAAACTTCCA; reverse, GTCAGCTCCCTGTTCTTTGC) were analyzed with SYBR Green using 18S (forward, GTAACCCGTTGAACCCCATT; reverse, CCATCCAATCGGTAGTAGCG) as housekeeping in an Eco Real-Time PCR System (Illumina, CA). The mRNA expression was quantified using the comparative CT method.

2.11 | Statistical analysis

Data were statistically analyzed using a *t* test or one-way analysis of variance with a post-hoc Bonferroni multiple-comparison test (Prism 8 for Mac). Differences were considered statistically significant at $p < .05$.

3 | RESULTS

3.1 | CA and deoxycholic acid induce an atrophic condition in C_2C_{12} myotubes

First, we analyzed the effect of CA and DCA on the viability of C_2C_{12} myotubes. Our results show that DCA (Figure 1a) and CA (Figure 1b) do not show a decrease in the myotube viability until 180 and 750 μM, respectively. The same figures show that DCA only shows a toxic effect at 240 μM, whereas CA does at 1000 μM.

Then, we evaluated if DCA and CA can induce an atrophic condition in vitro by a curve of doses evaluating the MHC protein levels (Figure S1A,C). Thus, we observed that the bile acids show an atrophic effect at 120 and 180 μM for DCA (Figure S1B) and 300 and 500 μM for CA (Figure S1D). Under these conditions, we evaluated the levels of three myofibrillar proteins: MHC (Figure 2), troponin (Figure 2d), and tropomyosin (Figure 2g) by western blot analysis. The quantifications and densitometric analysis of the experiments indicate that both DCA and CA decrease the MHC

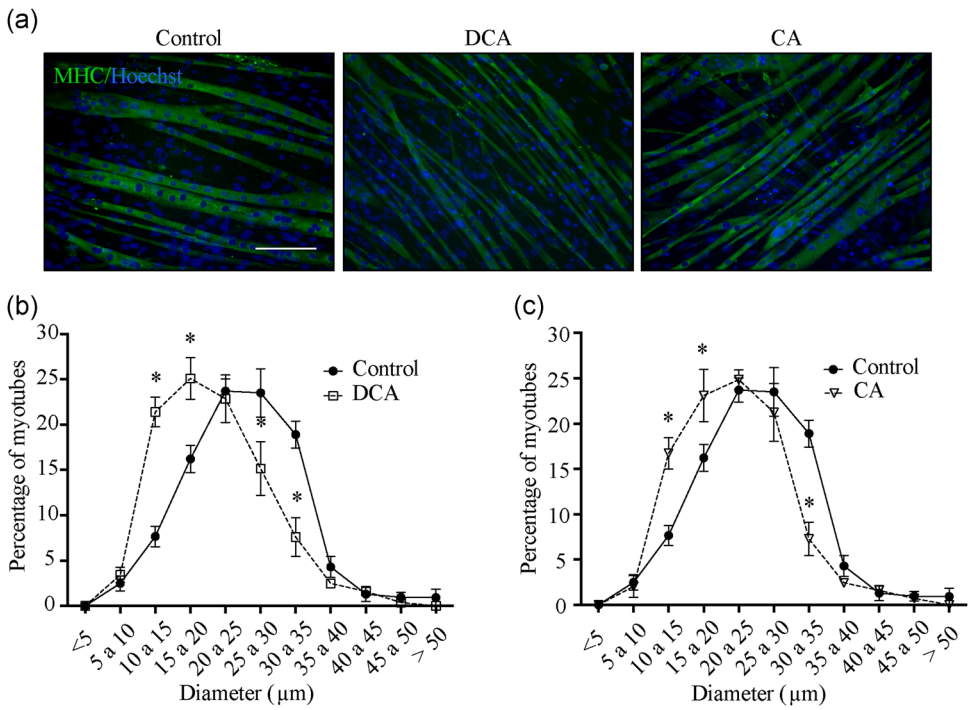

FIGURE 3 DCA and CA reduce the diameter of C_2C_{12} myotubes. Myotubes incubated with DCA (120 μM) or CA (500 μM) for 72 hr. (a) MHC was detected by indirect immunofluorescence and used to delimit the myotube area. Images were captured by microscopy, and the diameter of the myotubes was measured using ImageJ. The quantification was performed for DCA (b) or CA (c) and plotted. The values indicate the percentage of myotubes expressed as the mean ± *SEM* of three independent experiments in triplicate (one-way ANOVA, post-hoc Bonferroni, *$p < .05$ relative to the control). ANOVA, analysis of variance; CA, cholic acid; DCA, deoxycholic acid; MHC, myosin heavy chain

(Figure 2b,c), troponin (Figure 2e,f), and tropomyosin (Figure 2h,i) protein levels.

Further, we evaluated the effect of DCA and CA on the C_2C_{12} myotube diameter. Figure 3a shows the myotube diameter delineated by the detection of MHC through indirect immunofluorescence. The quantification of these data indicates that DCA (Figure 3b) and CA (Figure 3c) induce the displacement to the left in the size distribution of the myotubes compared with the control.

Together, these results indicate that DCA and CA induce an atrophic effect in C_2C_{12} myotubes.

3.2 | C_2C_{12} myotubes express the TGR5 receptor but not FXR for bile acids

We analyzed the expression of TGR5 and FXR receptor during C_2C_{12} differentiation. First, we evaluated gene expression. The results show that the FXR gene is not expressed during the different days of C_2C_{12} cell differentiation (Figure 4a). However, the TGR5 gene is expressed in C_2C_{12} myoblast (Day 0), which is increased at 3 and 6 days of differentiation (Figure 4b). Thus, we evaluated the TGR5 expression at the protein level during myogenesis. Figure 4c shows that levels of TGR5 increase at Day 2 (2.3 ± 0.4-fold compared with Day 0) and are maintained elevated at similar levels until Day 7 (3.0 ± 0.5-fold compared with Day 0; Figure 4d).

Thus, we can conclude that C_2C_{12} cells express the TGR5 receptor, which increases during skeletal muscle differentiation. In addition, C_2C_{12} cells do not express the FXR receptor.

3.3 | TGR5 activation with INT-777 agonist decreases skeletal muscle atrophy in C_2C_{12} myotubes

Since TGR5 is the bile acid receptor expressed in C_2C_{12} cells, we first evaluated the TGR5 activation through a plasmid reporter (pCre-luc) dependent on cAMP induced by TGR5. The results show that INT-777 increases the pCre-luc activity in a manner dependent on

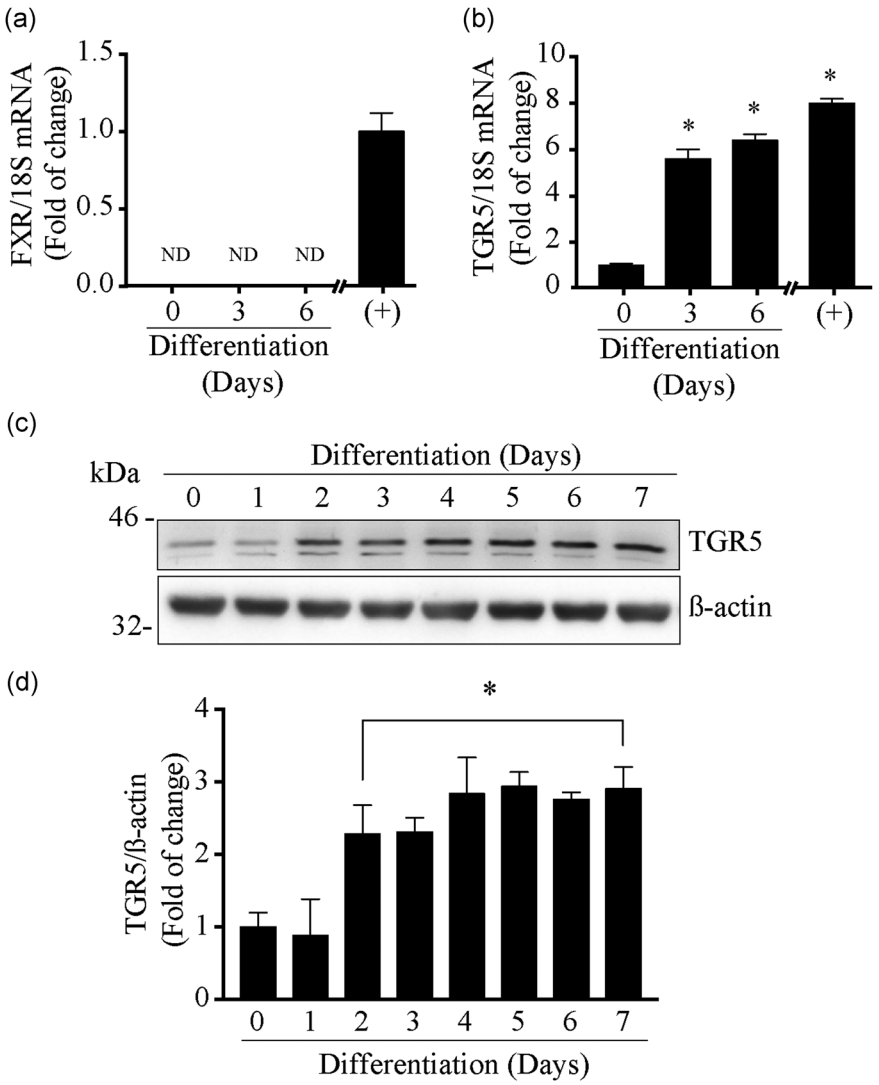

FIGURE 4 Expression of bile acid receptors in skeletal muscle cells. mRNA expression of bile acid receptors FXR (a) and TGR5 (b) was evaluated by RT-qPCR in C_2C_{12} cells undifferentiated (Day 0) or differentiated (Days 3 and 6) using 18S gene as housekeeping. cDNA from the liver extract was used as a positive control (+). (c) Protein levels of TGR5 were evaluated by western blot analysis in C_2C_{12} at different days of differentiation. β-Actin was used as loading control, and the molecular weights are shown in kDa. (d) Densitometric analysis of the bands in C is plotted. The values are shown as a fold of change and expressed as the mean ± *SD* of three independent experiments in triplicate (one-way ANOVA, post-hoc Bonferron, $^*p < .05$ relative to the Day 0). ANOVA, analysis of variance; cDNA, complementary DNA; FXR, farnesoid X receptor; mRNA, messenger RNA; RT-qPCR, reverse-transcription quantitative polymerase chain reaction

the dosage (Figure S2A). Similar results are shown for DCA (Figure S2B) and CA (Figure S2C).

Then, we analyzed the effect of TGR5 activator INT-777 on the atrophic condition in C_2C_{12} myotubes. Figure 5a shows that INT-777 qualitatively decreases the myotube diameter. The quantification of the data shows that INT-777 at 25 and 50 μM displaced the myotube size to the left, indicating a diminution of the diameter by TGR5 activation, with a more pronounced effect at 50 μM (Figure 5b).

Further, we evaluated the effect of INT-77 on the MHC protein levels by western blot analysis (Figure 5c). The results show that INT-777 decreases the MHC protein levels in a dose-dependent manner (Figure 5d), reaching a diminution similar to that shown by DCA and CA acids (Figure 3b,c).

3.4 | Skeletal muscle atrophy induced by DCA and CA is dependent on TGR5 receptor expression

To probe if TGR5 is involved in the effect of DCA and CA on muscle atrophy, we used a culture of EDL muscle fiber from WT and KO for TGR5 ($TGR5^{-/-}$) adult mice. In agreement with our results in C_2C_{12} myotubes, the diameter of muscle fibers from WT decreases when the muscle fibers are incubated with DCA and CA (Figure 6a, upper panel). The quantification of these data shows that DCA induces an increase of WT fiber percentage with a lower diameter and a decrease in the proportion of WT fiber with a higher diameter than control (Figure 6b). Similar results are shown for WT fibers when they are incubated with CA (Figure 6c). When the same experiments were done with muscle fibers from $TGR5^{-/-}$ mice (Figure 6a, lower panel), the change and

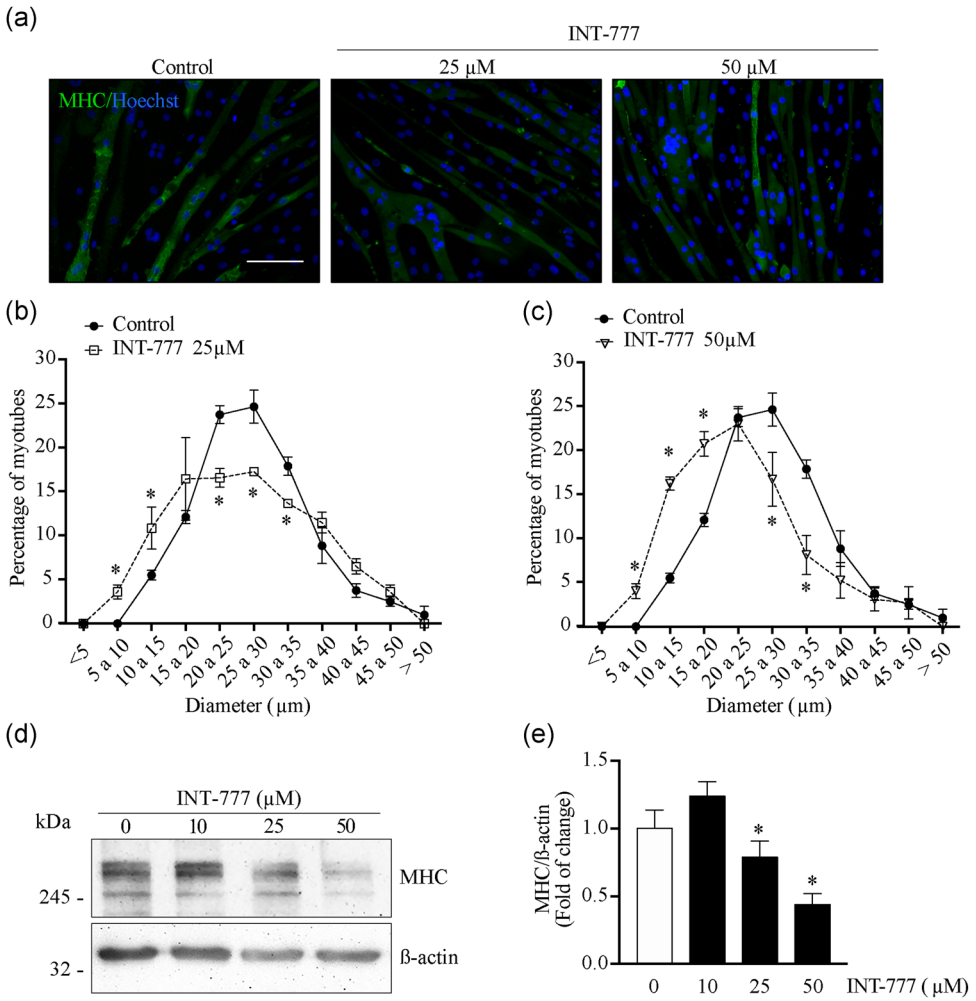

FIGURE 5 TGR5 agonist INT-777 reduces the diameter of the myotubes and the MHC protein levels in myotubes. C_2C_{12} myoblasts differentiated for 5 days were incubated with INT-777. (a) MHC was detected with indirect immunofluorescence and used to delimit the myotubes area. Microscopy images were captured and the diameter of the myotubes was measured using ImageJ. The effect of INT-777 at 25 μM (b) and 50 μM (c) was determined and the diameters of the myotubes were grouped in ranges and plotted. The values indicate the percentage of myotubes and were expressed as the mean ± *SEM* of three independent experiments in triplicate (one-way ANOVA, post-hoc Bonferroni, $^*p < .05$ relative to the control). (d) Protein levels of MHC were determined by western blot analysis. β-Actin is shown as loading control and molecular weight is indicated in kDa. (e) Densitometric analysis of the MHC bands. The values are shown as a fold of change and expressed as the mean ± *SD* of three independent experiments in triplicate (*t* test; $^*p < .05$ relative to the control). ANOVA, analysis of variance; MHC, myosin heavy chain

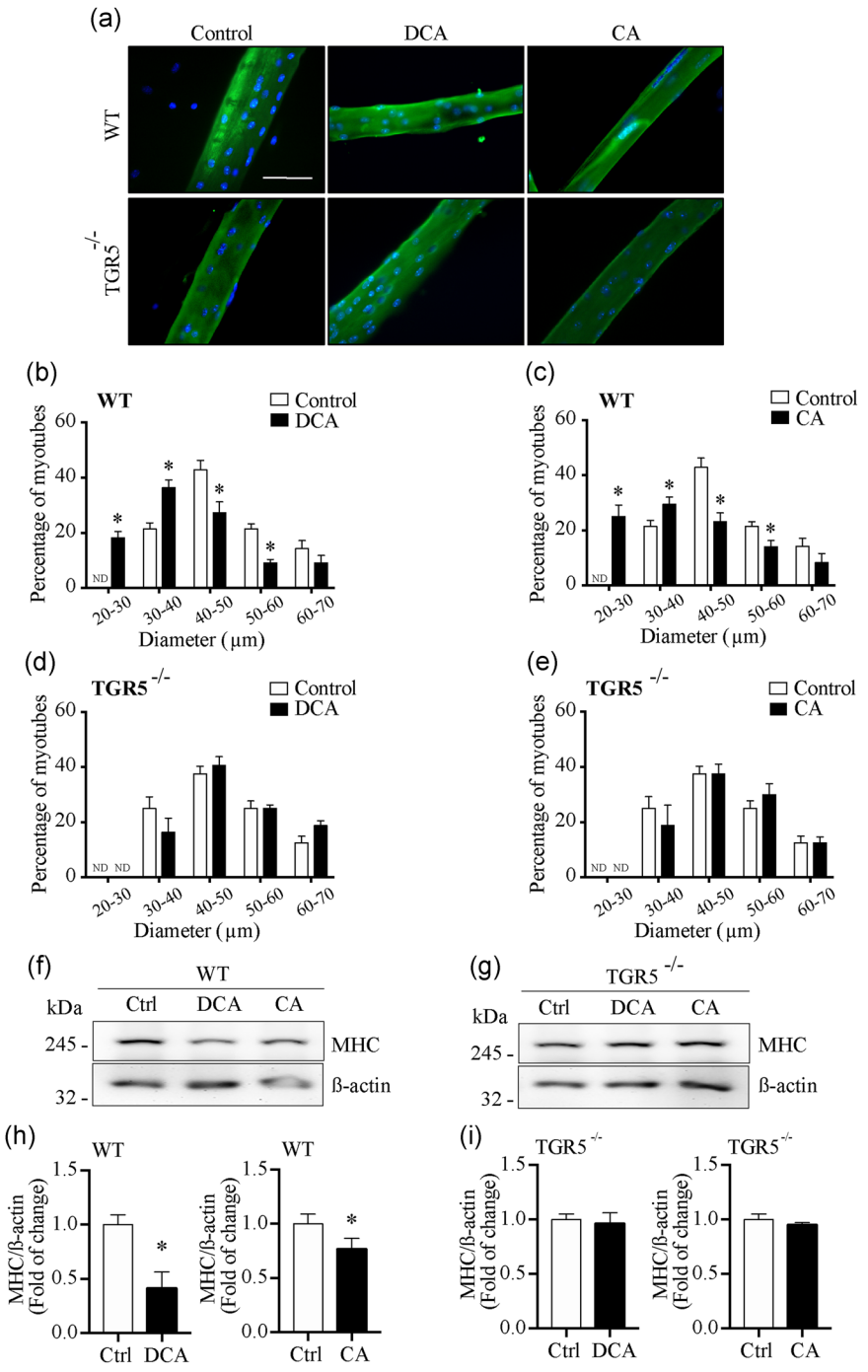

FIGURE 6 DCA and CA produce an atrophic effect in skeletal muscle fibers through TGR5 receptor. EDL muscle fibers were isolated from WT and TGR5$^{-/-}$ mice and incubated with DCA (120 μM) or CA (500 μM) for 72 hr. (a) MHC was detected by indirect immunofluorescence and used to delimit the fiber area. Microscopy images were captured, and the diameter was measured using ImageJ. The fiber diameters were grouped in ranges and plotted as the percentage of WT fibers incubated with DCA (b) or CA (c), and for fibers TGR5$^{-/-}$ incubated with DCA (d) or CA (e). The values indicate the mean ± *SD* of three independent experiments in triplicate (one-way ANOVA, post-hoc Bonferron, $^{*}p < .05$ relative to the control). Protein levels of MHC in WT (f) and TGR5$^{-/-}$ (g) fibers were determined by western blot analysis, with β-actin as a loading control and molecular weight shown in kDa. Densitometric analysis of the MHC bands in WT (h) and TGR5$^{-/-}$ (i). The values are shown as a fold of change and expressed as the mean ± *SD* of three independent experiments in triplicate (*t* test. $^{*}p < .05$ relative to the control). ANOVA, analysis of variance; CA, cholic acid; DCA, deoxycholic acid; EDL, extensor digitorum longus; MHC, myosin heavy chain; WT, wild type

displacement to the left in the diameter size of the fiber were totally prevented for both DCA (Figure 6d) and CA (Figure 6e).

In addition, we evaluated the MHC protein levels by western blot analysis in muscle fiber from WT and TGR5$^{-/-}$ mice (Figure 5c). The results of the western blot analysis for MHC levels from WT fibers (Figure 6f) showed a decrease of 58.7 ± 15% and 23.3 ± 10% for DCA and CA, respectively (Figure 6g). However, no changes were observed when the muscle fibers from TGR5$^{-/-}$ mice were incubated with DCA and CA (Figure 6h), reaching MHC levels similar to the control (Figure 6i).

Together, the results above suggest that TGR5 is required for DCA and CA to produce an atrophic condition in skeletal muscle fibers.

3.5 | Deoxycholic and CAs induce an increment of protein catabolic pathways as well as oxidative stress through a TGR5-dependent mechanism

We evaluated the effect of DCA and CA, and the TGR5 participation, on the expression of atrogin-1 and MuRF-1, two muscle-specific

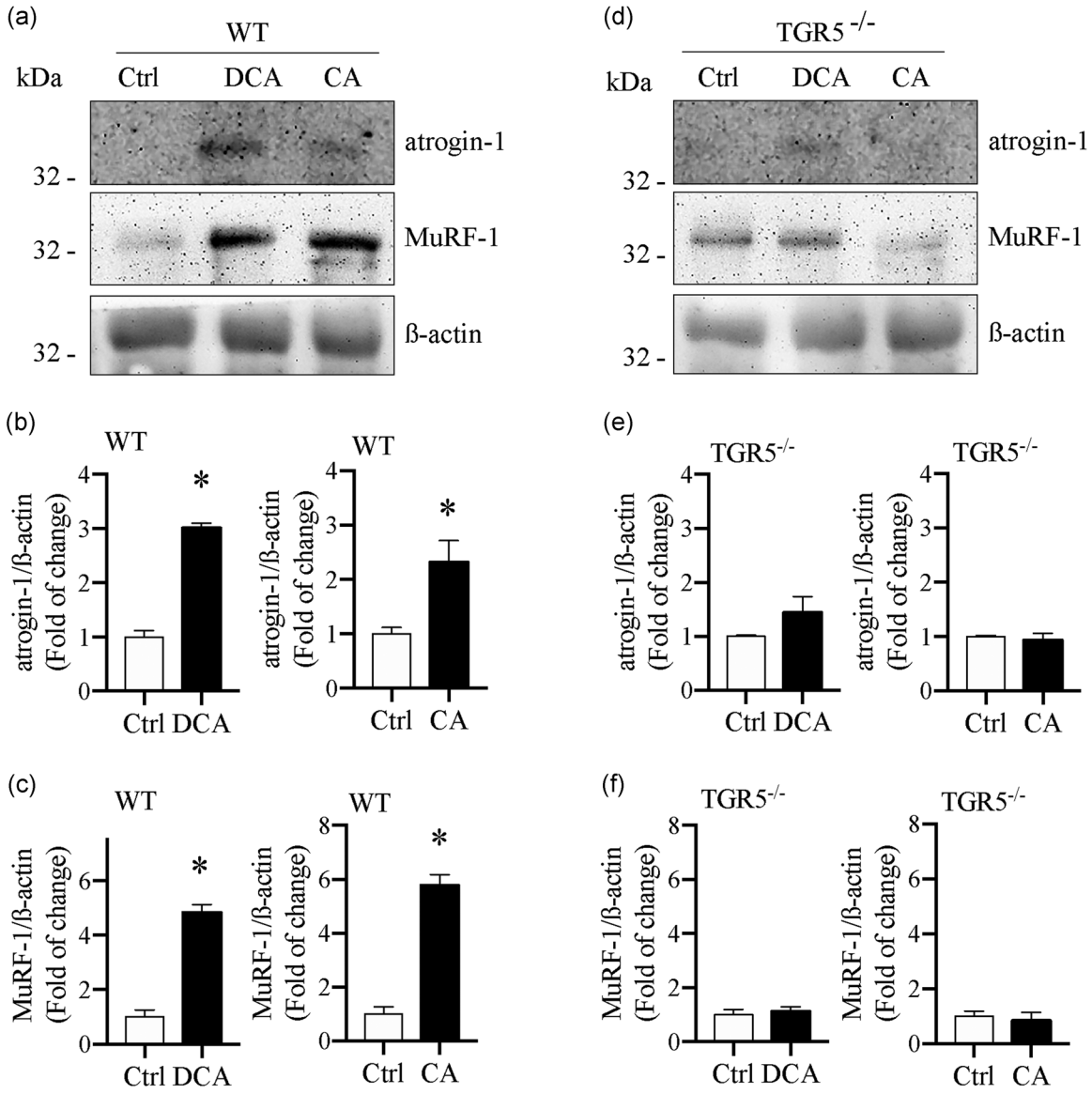

FIGURE 7 Atrogin-1 and MuRF-1 protein levels are increased by DCA and CA through TGR5 receptor in muscle fibers. EDL muscle fibers were isolated from WT and TGR5$^{-/-}$ mice and incubated with DCA (120 μM) or CA (500 μM) for 72 hr. Protein levels of atrogin-1 and MuRF-1 were determined by western blot analysis in WT (a) and TGR5$^{-/-}$ (d) fibers, with β-actin as the loading control. Molecular weights are shown in kDa. Densitometric analysis was performed for atrogin-1 in WT (b) and TGR5$^{-/-}$ (e) fibers, and for MuRF-1 in WT (c) and TGR5$^{-/-}$ (f) fibers. The values are shown as a fold of change and expressed as the mean ± *SD* of three independent experiments in triplicate (one-way ANOVA, post-hoc Bonferron, *$p < .05$ relative to the control). ANOVA, analysis of variance; CA, cholic acid; DCA, deoxycholic acid; EDL, extensor digitorum longus; WT, wild type

E3-ubiquitin ligases increased in muscle atrophy. Figure 7a shows that DCA and CA augment the atrogin-1 and MuRF-1 protein levels in WT muscle fibers. The quantification of these data indicates that DCA and CA increase atrogin-1 (Figure 7b; 3.0 ± 0.1-fold and 2.3 ± 0.4-fold, respectively). Also, DCA and CA increment MuRF-1 levels (Figure 7c; 4.8 ± 0.3-fold and 5.8 ± 0.4-fold, respectively). The results from Figure 7d show the protein levels of atrogin-1 and MuRF-1 in muscle fibers from TGR5$^{-/-}$ mice incubated with DCA and CA. The results show that DCA and CA do not change the protein levels of atrogin-1 (Figure 7e) or MuRF-1 (Figure 7f) in TGR5$^{-/-}$ fibers. Besides, we also evaluated the effect of DCA and CA on autophagy. Our results show that LC3II/LC3I ratio increases with DCA and CA (Figure S3A,B; 2.2 ± 0.4-fold and 1.8 ± 0.2-fold, respectively), while p62 protein levels decrease under DCA and CA incubation in C_2C_{12} myotubes (Figure S3C,D; 42.7 ± 10.1% and 52.0 ± 6.9%, respectively).

As ROS is implicated in several forms of skeletal muscle atrophy, ROS production was assessed in WT and TGR5$^{-/-}$ muscle fibers exposed to DCA and CA. Figure 8a shows the ROS detection through DCF fluorescence. The quantification of the data indicates that, in WT fibers, the increment of ROS production by DCA and CA was 4.2 ± 0.3-fold and 3.1 ± 0.3-fold, respectively (Figure 8b). In TGR5$^{-/-}$ fibers,

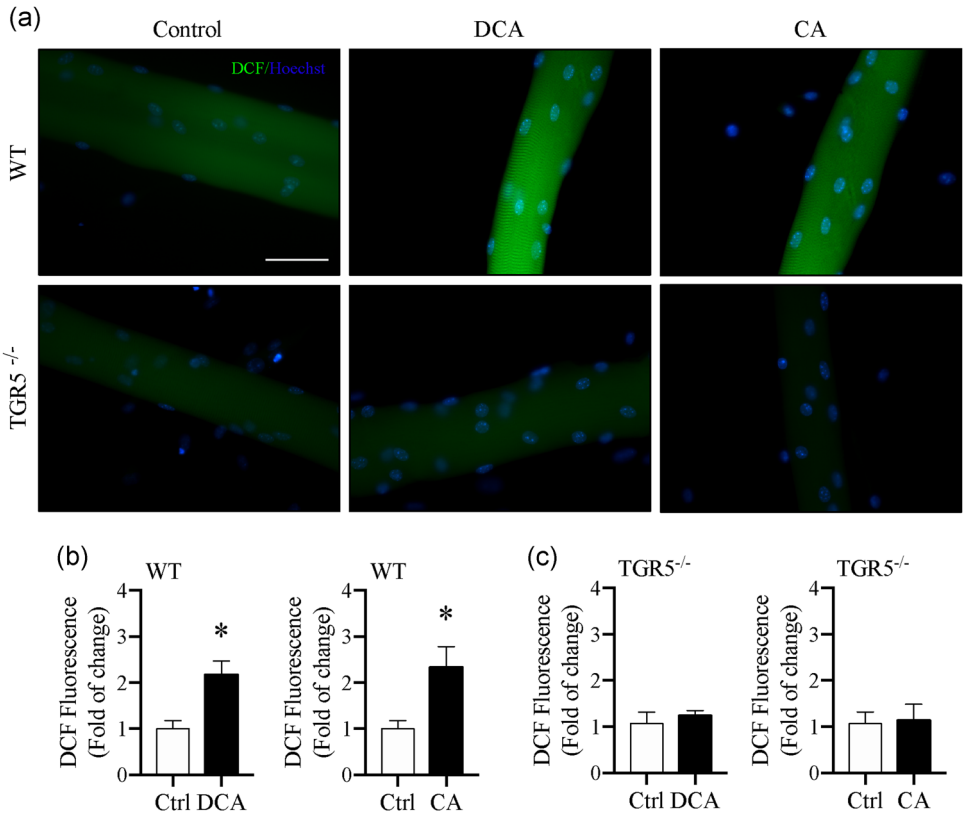

FIGURE 8 DCA and CA through TGR5 receptor increase the ROS levels in skeletal muscle fibers. Skeletal muscle fibers isolated from EDL muscle of WT and TGR5$^{-/-}$ mice were incubated with DCA (120 μM) or CA (500 μM) for 24 hr. (a) ROS levels in the fibers were detected with the CM-H2-DCF-DA dye (nuclei were stained with Hoechst). The green fluorescence intensity in the fiber area was determined and was indicated for WT (b) and TGR5$^{-/-}$ (c) fibers. The values are shown as the mean of the fold change ± *SD* of three independent experiments (one-way ANOVA, post-hoc Bonferroni, $^{*}p < .05$ relative to the control). ANOVA, analysis of variance; CA, cholic acid; DCA, deoxycholic acid; ROS, reactive oxygen species

there is no induction of ROS production by DCA or CA (Figure 8c). To corroborate the oxidative stress participation in the effect of DCA and CA, we evaluated the protein modifications by 4-HNE adducts. Our results, as shown in Figure 9a, indicate that DCA (Figure 9c; 2.2 ± 0.1-fold) and CA (Figure 9d; 1.8 ± 0.1-fold) increase the 4-HNE reactivity compared with control in WT fibers. Figure 9b shows that in TGR5$^{-/-}$ fibers, the effect of DCA (Figure 9e) and CA (Figure 9f) was lost (1.3 ± 0.4-fold and 1.1 ± 0.3-fold, respectively).

These results indicate that DCA and CA can increase the expression of markers of UPS, autophagy, and oxidative stress through a TGR5-dependent mechanism in skeletal muscle fibers.

4 | DISCUSSION

In this paper, we have demonstrated that DCA and CA bile acids induce an atrophic condition in skeletal muscle fibers and C_2C_{12} myotubes. Besides, we have demonstrated that this effect is dependent on TGR5 receptor expression.

In general, few antecedents of the role of bile acids in skeletal muscle have been described. Thus, bile acids, through the TGR5 receptor, participate in the regulation of metabolic activity and energy expenditure by the induction of deiodinase 2 expression (Watanabe et al., 2006). In addition, a specific TGR5 agonist decreases insulin resistance in skeletal muscles and improves glucose homeostasis in diabetic mice (Huang et al., 2019). Recently, it was described that TGR5 could regulate the muscle mass-producing hypertrophy (Sasaki et al., 2018). This antecedent contrasts with our results and can be explained because this paper used a transgenic mouse to overexpresses TGR5. Therefore, the effects of taurolithocholic acid published in this paper are not observed in mice with endogenous levels of the TGR5 receptor (Sasaki et al., 2018). Our data showed, for the first time, an atrophic effect of DCA and CA bile acids on muscle fibers or differentiated myotubes with endogenous levels of TGR5 receptor. Interestingly, our data are also supported by the atrophic effect observed when TGR5 agonist INT-777 was used, and with the loss of atrophic condition when TGR5$^{-/-}$ fibers were incubated with DCA and CA.

Our data indicated that TGR5 activation induces an increment in ROS production and 4-HNE modification on proteins, which is in line with the idea of increased oxidative stress. Moreover, we have recently described that N-acetyl cysteine treatment of mice with cholestatic CLD (with high plasma levels of bile acids) prevented the development of oxidative stress and diminution of muscle strength (Abrigo, Marin,

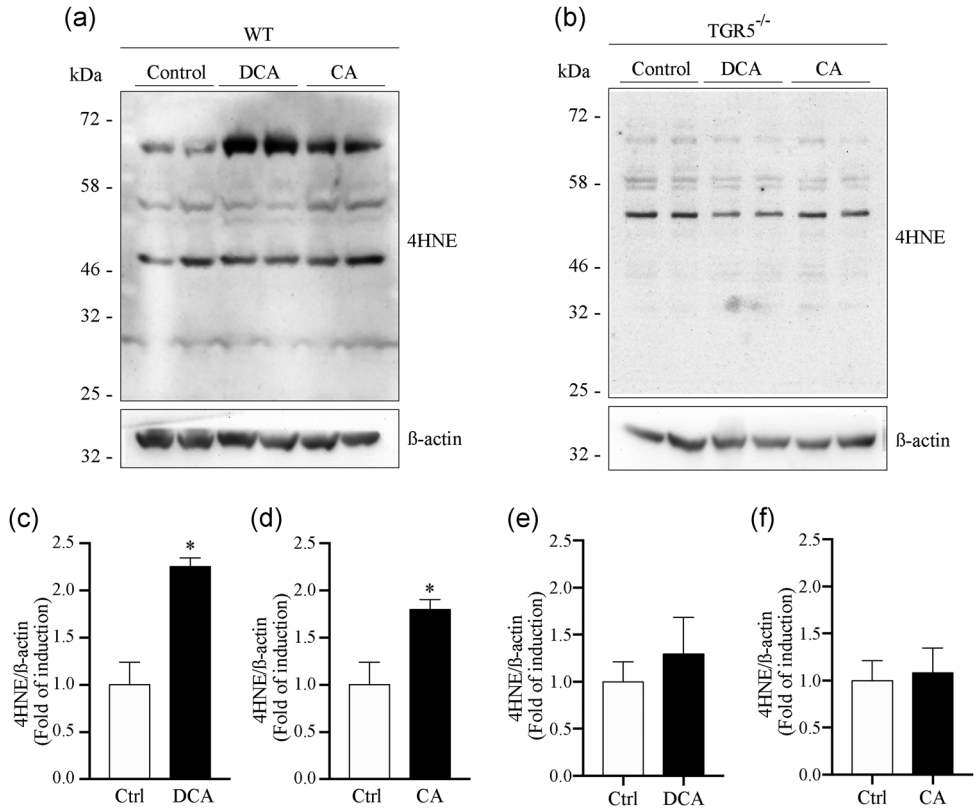

FIGURE 9 DCA and CA increase the protein oxidation levels through TGR5 receptor in skeletal muscle fibers. Skeletal muscle fibers isolated from EDL muscle of WT and TGR5$^{-/-}$ mice were incubated with DCA (120 μM) or CA (500 μM) for 72 hr. (a, b) Levels of oxidation-dependent 4-HNE protein adducts were detected by western blot analysis using anti-4-HNE antibody. β-Actin levels were used as loading control. Molecular weights are shown in kDa. Quantitative analysis based in the densitometry of the bands was performed for WT-DCA (c) and WT-CA (d), as well for TGR5$^{-/-}$-DCA (e) and TGR5$^{-/-}$-DCA (f). The values are shown as a fold of change and expressed as the mean ± *SD* of three independent experiments (one-way ANOVA, post-hoc Bonferron, $^{*}p < .05$ relative to the control)

et al., 2019). There are antecedents that TGR5 activation is involved in the generation of oxidative stress in hepatic, breast cancer, and esophageal adenocarcinoma cells (Gonzalez-Sanchez et al., 2016; Kovacs et al., 2019; Li & Cao, 2016). We must perform other studies about the effect of DCA and CA on the activity of antioxidant machinery to correlate with oxidative stress and also determine the source of ROS production stimulated by DCA and CA.

The increment in ROS production correlates with an increase in MuRF-1 and atrogin-1 expression. Other authors and we have shown that these muscle-specific E3 ligases are typical markers of muscle atrophy and indicators of UPS overactivation (Abrigo et al., 2016; Attaix et al., 2005; Campos et al., 2018; Morales et al., 2015). Also, an increment in UPS activity and autophagy correlates with a decrease in myofibrillar proteins, such as MHC and troponin, observed in our data. Our data is the first report that the bile acids, DCA and CA, induce an increase in UPS and autophagy components associated with muscle atrophy. These results are in agreement with a report that bile acids cause the degradation of bile acid transporter via UPS from ileum and impaired autophagy in the liver (Kim et al., 2018; Miyata et al., 2013). Thus, our results suggest that DCA and CA could be stimulating the protein breakdown in skeletal muscle and thus contributing to muscle wasting.

Several studies indicate that skeletal muscles express only TGR5 as a receptor for bile acids (Sasaki et al., 2018; Watanabe et al., 2006). However, the data for the FXR receptor is not available or is not directly shown. Thus, we have probed that skeletal muscle cells do not express FXR. Moreover, we have shown that TGR5 increases its expression during myogenesis in vitro. Our data is in agreement with the study in which TGR5 overexpression suggests that this receptor enhances muscle differentiation in C_2C_{12} cells (Sasaki et al., 2018). However, more analysis must be performed to elucidate the possible participation of myogenic regulatory factors or other transcription factors in the increased expression of TGR5 gene during skeletal muscle differentiation. In skeletal muscle, TGR5 has been described as a receptor that can be regulated by exercise through a mechanism dependent on the activating transcription factor 6 (ATF6) and UPR (Sasaki et al., 2018).

5 | CONCLUSIONS

In summary, in this paper, we have shown for the first time that CA and DCA, in a form dependent on TGR5 expression, induce an

atrophic condition in skeletal muscle fibers, concomitant with increased levels of oxidative stress and protein catabolic pathways.

ACKNOWLEDGMENTS

The design of the study, collection, analysis, interpretation of the data, and writing of the manuscript was supported by research grants from the National Fund for Science and Technological Development (FONDECYT 1161646 [CCV], 1161288 [FS]; 11171001 [DC]), Millennium Institute on Immunology and Immunotherapy (P09-016-F [CCV, FS]), Programa de Cooperación Científica ECOS-CONICYT (C16S02 [CCV]), Basal Grant CEDENNA (AFB180001 [CCV]), and Center for Aging and Regeneration (CARE CONICYT AFB170005 [MA]). J. Ábrigo thank CONICYT for providing a Ph.D. scholarship (21161353). The Millennium Nucleus of Ion Channels-Associated Diseases (MiNICAD) is a Millennium Nucleus supported by the Iniciativa Científica Milenio of the Ministry of Economy, Development and Tourism (Chile).

CONFLICT OF INTERESTS

The authors declare that there are no conflict of interests.

AUTHOR CONTRIBUTIONS

J. A., F. G., A. G., F. T., D. C., and F. A. were responsible for carrying out the experiments and analyzing the data. C. C. V., M. A., S. K., and F. S. were involved in interpreting and drafting of the manuscript for publication. C. C. V. was responsible for conceiving all the experiments and was also involved in analyzing and preparing the data for publication and drafting of the manuscript.

DATA AVAILABILITY STATEMENT

The data that support the findings of this study are available from the corresponding author on reasonable request.

ETHICS STATEMENT

All protocols were conducted in strict accordance and with the formal approval of the Animal Ethics Committee at the Universidad Andrés Bello (Approval number 007/2016).

ORCID

Claudio Cabello-Verrugio http://orcid.org/0000-0001-7273-2102

REFERENCES

Abrigo, J., Elorza, A. A., Riedel, C. A., Vilos, C., Simon, F., Cabrera, D., … Cabello-Verrugio, C. (2018). Role of oxidative stress as key regulator of muscle wasting during cachexia. *Oxidative Medicine and Cellular Longevity*, *2018*, 2063179–17. https://doi.org/10.1155/2018/2063179

Abrigo, J., Marin, T., Aguirre, F., Tacchi, F., Vilos, C., Simon, F., … Cabello-Verrugio, C. (2019). N-Acetyl Cysteine attenuates the sarcopenia and muscle apoptosis induced by chronic liver disease. *Current Molecular Medicine*, *20*, 60–71. https://doi.org/10.2174/1566524019666190917124636

Abrigo, J., Rivera, J. C., Aravena, J., Cabrera, D., Simon, F., Ezquer, F., … Cabello-Verrugio, C. (2016). High fat diet-induced skeletal muscle wasting is decreased by mesenchymal stem cells administration: implications on oxidative stress, ubiquitin proteasome pathway activation, and myonuclear apoptosis. *Oxidative Medicine and Cellular Longevity*, *2016*, 9047821–13. https://doi.org/10.1155/2016/9047821

Abrigo, J., Simon, F., Cabrera, D., Vilos, C., & Cabello-Verrugio, C. (2019). Mitochondrial dysfunction in skeletal muscle pathologies. *Current Protein & Peptide Science*, *20*(6), 536–546. https://doi.org/10.2174/1389203720666190402100902

Attaix, D., Ventadour, S., Codran, A., Bechet, D., Taillandier, D., & Combaret, L. (2005). The ubiquitin-proteasome system and skeletal muscle wasting. *Essays in Biochemistry*, *41*, 173–186. https://doi.org/10.1042/EB0410173

Bilodeau, P. A., Coyne, E. S., & Wing, S. S. (2016). The ubiquitin proteasome system in atrophying skeletal muscle: Roles and regulation. *American Journal of Physiology: Cell Physiology*, *311*(3), C392–C403. https://doi.org/10.1152/ajpcell.00125.2016

Cabello-Verrugio, C., Acuna, M. J., Morales, M. G., Becerra, A., Simon, F., & Brandan, E. (2011). Fibrotic response induced by angiotensin-II requires NAD(P)H oxidase-induced reactive oxygen species (ROS) in skeletal muscle cells. *Biochemical and Biophysical Research Communications*, *410*(3), 665–670. https://doi.org/10.1016/j.bbrc.2011.06.051

Cabello-Verrugio, C., Rivera, J. C., & Garcia, D. (2017). Skeletal muscle wasting: New role of nonclassical renin-angiotensin system. *Current Opinion in Clinical Nutrition and Metabolic Care*, *20*(3), 158–163. https://doi.org/10.1097/MCO.0000000000000361

Call, J. A., & Nichenko, A. S. (2020). Autophagy: An essential but limited cellular process for timely skeletal muscle recovery from injury. *Autophagy*, 1–4. https://doi.org/10.1080/15548627.2020.1753000

Campos, F., Abrigo, J., Aguirre, F., Garces, B., Arrese, M., Karpen, S., … Cabello-Verrugio, C. (2018). Sarcopenia in a mice model of chronic liver disease: Role of the ubiquitin-proteasome system and oxidative stress. *Pflugers Archiv. European Journal of Physiology*, *470*(10), 1503–1519. https://doi.org/10.1007/s00424-018-2167-3

Cao, R. Y., Li, J., Dai, Q., Li, Q., & Yang, J. (2018). Muscle atrophy: Present and future. *Advances in Experimental Medicine and Biology*, *1088*, 605–624. https://doi.org/10.1007/978-981-13-1435-3_29

Dasarathy, S. (2013). Posttransplant sarcopenia: An underrecognized early consequence of liver transplantation. *Digestive Diseases and Sciences*, *58*(11), 3103–3111. https://doi.org/10.1007/s10620-013-2791-x

Deutschmann, K., Reich, M., Klindt, C., Droge, C., Spomer, L., Haussinger, D., & Keitel, V. (2018). Bile acid receptors in the biliary tree: TGR5 in physiology and disease. *Biochimica et Biophysica Acta (BBA)—Molecular Basis of Disease*, *1864*, 1319–1325. https://doi.org/10.1016/j.bbadis.2017.08.021

Ding, S., Dai, Q., Huang, H., Xu, Y., & Zhong, C. (2018). An overview of muscle atrophy. *Advances in Experimental Medicine and Biology*, *1088*, 3–19. https://doi.org/10.1007/978-981-13-1435-3_1

Dossa, A. Y., Escobar, O., Golden, J., Frey, M. R., Ford, H. R., & Gayer, C. P. (2016). Bile acids regulate intestinal cell proliferation by modulating EGFR and FXR signaling. *American Journal of Physiology. Gastrointestinal and Liver Physiology*, *310*(2), G81–G92. https://doi.org/10.1152/ajpgi.00065.2015

Droguett, R., Cabello-Verrugio, C., Santander, C., & Brandan, E. (2010). TGF-beta receptors, in a Smad-independent manner, are required for terminal skeletal muscle differentiation. *Experimental Cell Research*, *316*(15), 2487–2503. https://doi.org/10.1016/j.yexcr.2010.04.031

Dumitru, A., Radu, B. M., Radu, M., & Cretoiu, S. M. (2018). Muscle changes during atrophy. *Advances in Experimental Medicine and Biology*, *1088*, 73–92. https://doi.org/10.1007/978-981-13-1435-3_4

Englesbe, M. J., Patel, S. P., He, K., Lynch, R. J., Schaubel, D. E., Harbaugh, C., … Sonnenday, C. J. (2010). Sarcopenia and mortality after liver transplantation. *Journal of the American College of Surgeons*, *211*(2), 271–278. https://doi.org/10.1016/j.jamcollsurg.2010.03.039

Gonzalez-Sanchez, E., Perez, M. J., Nytofte, N. S., Briz, O., Monte, M. J., Lozano, E., … Marin, J. J. G. (2016). Protective role of biliverdin against bile acid-induced oxidative stress in liver cells. *Free Radical Biology and*

Medicine, *97*, 466–477. https://doi.org/10.1016/j.freeradbiomed.2016.06.016

Huang, S., Ma, S., Ning, M., Yang, W., Ye, Y., Zhang, L., … Leng, Y. (2019). TGR5 agonist ameliorates insulin resistance in the skeletal muscles and improves glucose homeostasis in diabetic mice. *Metabolism: Clinical and Experimental*, *99*, 45–56. https://doi.org/10.1016/j.metabol.2019.07.003

Kars, M., Yang, L., Gregor, M. F., Mohammed, B. S., Pietka, T. A., Finck, B. N., … Klein, S. (2010). Tauroursodeoxycholic Acid may improve liver and muscle but not adipose tissue insulin sensitivity in obese men and women. *Diabetes*, *59*(8), 1899–1905. https://doi.org/10.2337/db10-0308

Kawamata, Y., Fujii, R., Hosoya, M., Harada, M., Yoshida, H., Miwa, M., … Fujino, M. (2003). A G protein-coupled receptor responsive to bile acids. *Journal of Biological Chemistry*, *278*(11), 9435–9440. https://doi.org/10.1074/jbc.M209706200

Keitel, V., Stindt, J., & Haussinger, D. (2019). Bile acid-activated receptors: GPBAR1 (TGR5) and other G protein-coupled receptors. *Handbook of Experimental Pharmacology*, *256*, 19–49. https://doi.org/10.1007/164_2019_230

Khalil, R. (2018). Ubiquitin-proteasome pathway and muscle atrophy. *Advances in Experimental Medicine and Biology*, *1088*, 235–248. https://doi.org/10.1007/978-981-13-1435-3_10

Kim, M. J., & Suh, D. J. (1986). Profiles of serum bile acids in liver diseases. *Korean Journal of Internal Medicine*, *1*(1), 37–42. https://doi.org/10.3904/kjim.1986.1.1.37

Kim, S., Han, S. Y., Yu, K. S., Han, D., Ahn, H. J., Jo, J. E., … Park, H. W. (2018). Impaired autophagy promotes bile acid-induced hepatic injury and accumulation of ubiquitinated proteins. *Biochemical and Biophysical Research Communications*, *495*(1), 1541–1547. https://doi.org/10.1016/j.bbrc.2017.11.202

Kobayashi, Y., Hara, N., Sugimoto, R., Mifuji-Moroka, R., Tanaka, H., Eguchi, A., … Taguchi, O. (2017). The Associations between circulating bile acids and the muscle volume in patients with non-alcoholic fatty liver disease (NAFLD). *Internal Medicine*, *56*(7), 755–762. https://doi.org/10.2169/internalmedicine.56.7796

Kovacs, P., Csonka, T., Kovacs, T., Sari, Z., Ujlaki, G., Sipos, A., … Miko, E. (2019). Lithocholic acid, a metabolite of the microbiome, increases oxidative stress in breast cancer. *Cancers*, *11*(9), https://doi.org/10.3390/cancers11091255

Li, D., & Cao, W. (2016). Bile acid receptor TGR5, NADPH Oxidase NOX5-S and CREB mediate bile acid-induced DNA damage in Barrett's esophageal adenocarcinoma cells. *Scientific Reports*, *6*, 31538. https://doi.org/10.1038/srep31538

Li, T., & Apte, U. (2015). Bile acid metabolism and signaling in cholestasis, inflammation, and cancer. *Advances in Pharmacology*, *74*, 263–302. https://doi.org/10.1016/bs.apha.2015.04.003

Li, T., & Chiang, J. Y. (2015). Bile acids as metabolic regulators. *Current Opinions in Gastroenterology*, *31*(2), 159–165. https://doi.org/10.1097/MOG.0000000000000156

Luo, L., Aubrecht, J., Li, D., Warner, R. L., Johnson, K. J., Kenny, J., & Colangelo, J. L. (2018). Assessment of serum bile acid profiles as biomarkers of liver injury and liver disease in humans. *PLOS One*, *13*(3), e0193824. https://doi.org/10.1371/journal.pone.0193824

Makishima, M., Okamoto, A. Y., Repa, J. J., Tu, H., Learned, R. M., Luk, A., … Shan, B. (1999). Identification of a nuclear receptor for bile acids. *Science*, *284*(5418), 1362–1365. https://doi.org/10.1126/science.284.5418.1362

Meneses, C., Morales, M. G., Abrigo, J., Simon, F., Brandan, E., & Cabello-Verrugio, C. (2015). The angiotensin-(1-7)/Mas axis reduces myonuclear apoptosis during recovery from angiotensin II-induced skeletal muscle atrophy in mice. *Pflugers Archiv: European Journal of Physiology*, *467*(9), 1975–1984. https://doi.org/10.1007/s00424-014-1617-9

Miyata, M., Yamakawa, H., Hayashi, K., Kuribayashi, H., Yamazoe, Y., & Yoshinari, K. (2013). Ileal apical sodium-dependent bile acid transporter protein levels are down-regulated through ubiquitin-dependent protein degradation induced by bile acids. *European Journal of Pharmacology*, *714*(1-3), 507–514. https://doi.org/10.1016/j.ejphar.2013.06.036

Morales, M. G., Olguin, H., Di Capua, G., Brandan, E., Simon, F., & Cabello-Verrugio, C. (2015). Endotoxin-induced skeletal muscle wasting is prevented by angiotensin-(1-7) through a p38 MAPK-dependent mechanism. *Clinical Science*, *129*(6), 461–476. https://doi.org/10.1042/CS20140840

Painemal, P., Acuna, M. J., Riquelme, C., Brandan, E., & Cabello-Verrugio, C. (2013). Transforming growth factor type beta 1 increases the expression of angiotensin II receptor type 2 by a SMAD- and p38 MAPK-dependent mechanism in skeletal muscle. *Biofactors*, *39*(4), 467–475. https://doi.org/10.1002/biof.1087

Pasut, A., Jones, A. E., & Rudnicki, M. A. (2013). Isolation and culture of individual myofibers and their satellite cells from adult skeletal muscle. *Journal of Visualized Experiments*, *73*, e50074. https://doi.org/10.3791/50074

Ponziani, F. R., & Gasbarrini, A. (2017). Sarcopenia in patients with advanced liver disease. *Current Protein & Peptide Science*, https://doi.org/10.2174/1389203718666170428121647

Qi, Y., Jiang, C., Cheng, J., Krausz, K. W., Li, T., Ferrell, J. M., … Chiang, J. Y. (2015). Bile acid signaling in lipid metabolism: Metabolomic and lipidomic analysis of lipid and bile acid markers linked to anti-obesity and anti-diabetes in mice. *Biochimica et Biophysica Acta/General Subjects*, *1851*(1), 19–29. https://doi.org/10.1016/j.bbalip.2014.04.008

Sandri, M. (2010). Autophagy in skeletal muscle. *FEBS Letters*, *584*(7), 1411–1416. https://doi.org/10.1016/j.febslet.2010.01.056

Sandri, M. (2013). Protein breakdown in muscle wasting: Role of autophagy-lysosome and ubiquitin-proteasome. *International Journal of Biochemistry and Cell Biology*, *45*(10), 2121–2129. https://doi.org/10.1016/j.biocel.2013.04.023

Sasaki, T., Kuboyama, A., Mita, M., Murata, S., Shimizu, M., Inoue, J., … Sato, R. (2018). The exercise-inducible bile acid receptor Tgr5 improves skeletal muscle function in mice. *Journal of Biological Chemistry*, *293*(26), 10322–10332. https://doi.org/10.1074/jbc.RA118.002733

Shin, D. J., & Wang, L. (2019). Bile acid-activated receptors: A review on FXR and other nuclear receptors. *Handbook of Experimental Pharmacology*, *256*, 51–72. https://doi.org/10.1007/164_2019_236

Tsien, C., Garber, A., Narayanan, A., Shah, S. N., Barnes, D., Eghtesad, B., … Dasarathy, S. (2014). Post-liver transplantation sarcopenia in cirrhosis: A prospective evaluation. *Journal of Gastroenterology and Hepatology*, *29*(6), 1250–1257. https://doi.org/10.1111/jgh.12524

Watanabe, M., Houten, S. M., Mataki, C., Christoffolete, M. A., Kim, B. W., Sato, H., … Auwerx, J. (2006). Bile acids induce energy expenditure by promoting intracellular thyroid hormone activation. *Nature*, *439*(7075), 484–489. https://doi.org/10.1038/nature04330

SUPPORTING INFORMATION

Additional supporting information may be found online in the Supporting Information section.

How to cite this article: Abrigo J, Gonzalez F, Aguirre F, et al. Cholic acid and deoxycholic acid induce skeletal muscle atrophy through a mechanism dependent on TGR5 receptor. *J Cell Physiol*. 2020;1–13. https://doi.org/10.1002/jcp.29839